3-26-2008

SU(5) Grand Unification on a Domain-Wall Brane from an E_6-Invariant Action

Aharon Davidson
Ben-Gurion University

Damien P. George
The University of Melbourne

Archil Kobakhidze
The University of Melbourne

Raymond R. Volkas
The University of Melbourne

Kameshwar C. Wali
Syracuse University

Recommended Citation
arXiv:0710.3432v2

$SU(5)$ grand unification on a domain-wall brane from an E_6-invariant action

Aharon Davidson,[1,*] Damien P. George,[2,†] Archil Kobakhidze,[2,‡] Raymond R. Volkas,[2,§] and Kameshwar C. Wali[3,¶]

[1] *Physics Department, Ben-Gurion University, Beer-Sheva 84105, Israel*
[2] *School of Physics, Research Centre for High Energy Physics, The University of Melbourne, Victoria 3010, Australia*
[3] *Physics Department, Syracuse University, Syracuse NY 13244-1130, U.S.A.*

An $SU(5)$ grand unification scheme for effective $3+1$-dimensional fields dynamically localised on a domain-wall brane is constructed. This is achieved through the confluence of the clash-of-symmetries mechanism for symmetry breaking through domain-wall formation, and the Dvali-Shifman gauge-boson localisation idea. It requires an E_6 gauge-invariant action, yielding a domain-wall solution that has E_6 broken to differently embedded $SO(10) \otimes U(1)$ subgroups in the two bulk regions on opposite sides of the wall. On the wall itself, the unbroken symmetry is the intersection of the two bulk subgroups, and contains $SU(5)$. A $4+1$-dimensional fermion family in the 27 of E_6 gives rise to localised left-handed zero-modes in the $5^* \oplus 10 \oplus 1 \oplus 1$ representation of $SU(5)$. The remaining ten fermion components of the 27 are delocalised exotic states, not appearing in the effective $3+1$-dimensional theory on the domain-wall brane. The scheme is compatible with the type-2 Randall-Sundrum mechanism for graviton localisation; the single extra dimension is infinite.

PACS numbers:

I. INTRODUCTION

If our universe is a $3+1$-dimensional brane [1, 2, 3, 4, 5, 6, 7, 8, 9] existing in a $4+1$-dimensional spacetime, then the most likely field-theoretic origin for the brane is a scalar-field domain wall (DW) or kink [1]. This generic idea is naturally compatible with the type-2 Randall-Sundrum (RS2) mechanism for producing effective $3+1$-d gravity on the brane [9] (see, for example, Refs. [10, 11, 12] for the extension of thin-brane RS2 to a domain-wall brane). The challenge is to dynamically localise all the other ingredients necessary for a phenomenologically successful effective theory on the brane: gauge bosons, fermions, and Higgs bosons. Various localisation ideas for these disparate classes of fields have been recently combined to produce an effective brane theory that is plausibly very similar to the standard model [13].

The purpose of this paper is twofold. First, we wish to point out a very elegant generic connection between the clash-of-symmetries (CoS) mechanism for symmetry breaking through domain wall formation [14, 15, 16, 17][1], and the Dvali-Shifman (DS) idea for dynamical gauge-boson localisation [22]. Second, we use this remarkable confluence to construct an explicit scheme that realises an $SU(5)$ gauge-invariant effective theory on the brane. In a sense, it is a grand unified extension of the model of Ref. [13], but the way in which the Dvali-Shifman mechanism is realised is quite different, and we shall argue that it is in fact conceptually more advanced. Remarkably, this scheme immediately produces a realistic spectrum of localised fermion zero-modes [23] (for a review see [24]) using the simplest possible mechanism. While it is beyond the scope of this paper to write down a complete phenomenologically-acceptable domain-wall-brane localised $SU(5)$ theory, we shall conclude with brief remarks about how this could be attempted.

*Electronic address: davidson@bgu.ac.il
†Electronic address: d.george@physics.unimelb.edu.au
‡Electronic address: archilk@unimelb.edu.au
§Electronic address: raymondv@unimelb.edu.au
¶Electronic address: wali@phy.syr.edu

[1] See also [18, 19, 20] for related works, and [21] for soliton-induced supersymmetry breaking.

The clash-of-symmetries phenomenon [14, 15, 16, 17, 18, 19, 20] automatically arises when the simple Z_2 kink is extended to a theory with a continuous internal symmetry group G in addition to the discrete symmetry. Taking the scalar-field multiplet to be in a non-trivial representation of G, the domain-wall configuration spontaneously breaks G in addition to reflecting the disconnected vacuum manifold topology created by the spontaneous breaking of the discrete symmetry. Two classes of domain-wall solutions exist: those which respect the same subgroup H of G at all values of the bulk coordinate y, and those where the unbroken subgroup varies in the bulk. We shall call the first class "non-CoS domain walls", contrasted with the "CoS domain walls" of the second class. Clash-of-symmetries DWs can arise when the subgroups respected asymptotically (at $y = \pm\infty$) are isomorphic but *differently embedded* subgroups, H and H'. The symmetry group at finite y is typically the intersection $H \cap H'$, which is of course smaller than both H and H'.

The last observation provides an immediate connection with the Dvali-Shifman proposal for dynamical gauge-boson localisation. The DS mechanism, as originally proposed [22], envisaged a domain wall configuration where the full group G is restored in the bulk, but broken to H in the wall. The gauge bosons of H propagate on the wall either as massless Abelian gauge fields or glueballs formed from non-Abelian gauge fields. In the bulk, *all* gauge bosons have to be incorporated into massive G-glueballs.[2] Thus, the massless Abelian gauge fields on the wall have to become incorporated into massive glueballs in the bulk, and the energy cost associated with the mass gap then plausibly localises them to the wall. This heuristic argument is bolstered by the dual-superconductivity model [26, 27] for the confining bulk: the electric field lines from a source charge in the wall are repelled from the interface with the dual-superconducting bulk [28, 29], just as magnetic field lines are Meissner-repelled from an ordinary superconductor. The non-Abelian gauge fields of H are also plausibly localised if the mass of the G-glueballs exceeds the mass of the H-glueballs.

The fact that the full symmetry G is asymptotically restored is clearly not a necessary condition. In the CoS situation, the brane-group $H \cap H'$ is a subgroup of both H and H', the unbroken symmetries in the two semi-infinite bulk regions. By the DS reasoning, provided H and H' contain confining non-Abelian factors, at least some of the gauge bosons of $H \cap H'$ will be localised. For a realistic theory, we need the localised gauge bosons to include those of the standard model. The model-builder needs to engineer the theory to achieve this effect. While this engineering shall be the main concern in the rest of the paper, our first generic point has already been made: *the clash-of-symmetries automatically gives rise to Dvali-Shifman gauge-boson localisation.* This CoS alternative realisation of the DS mechanism seems conceptually neater than the original, because it can be achieved using scalars in a single irreducible representation of G. The original requires two multiplets: a G-singlet to form a kink, which in turn forces a G-multiplet to condense in the core of the wall.

We shall show that the CoS-DS confluence can naturally produce an $SU(5)$ effective theory on the brane. The basic ingredients are $G = E_6$, with the DW-producing scalar field in the adjoint or 78 representation. The groups H and H' will be the differently-embedded maximal subgroups $SO(10) \otimes U(1)_E$ and $SO(10)' \otimes U(1)_{E'}$, respectively. Their intersection is $SU(5) \otimes U(1) \otimes U(1)$, with $SU(5)$ of course being a subgroup of both $SO(10)$ and $SO(10)'$. Taking both of those as confining gauge theories in the bulk, the localisation of $SU(5)$ gauge bosons follows from the DS-effect. The gauge fields of $U(1) \otimes U(1)$ are *not* completely localised. When $4+1$-d fermions in the 27 of E_6 are Yukawa-coupled to the scalar multiplet, we shall show that $3+1$-d left-chiral zero-modes in the phenomenologically-realistic $5^* \otimes 10 \oplus 1 \oplus 1$ representation of $SU(5)$ are localised. The remaining ten fermion components remain $4+1$-d, and are thus absent from the effective brane-theory. The result that the chiralities of the zero-modes come out to be phenomenologically correct is very non-trivial, as we shall explain.

We review the clash-of-symmetries idea in Sec.II. Section III describes a warm-up example featuring $SO(10)$ CoS

---

[2] The Dvali-Shifman mechanism requires a confining $4+1$-dimensional gauge theory to live in the bulk. The issue of confinement in $4+1$ dimensions is not completely understood, so the Dvali-Shifman mechanism in that context has the status of being a plausible conjecture. There is good lattice gauge theory evidence that pure $SU(2)$ Yang-Mills theory with an ultraviolet cut-off is confining in $4+1$ dimensions when the gauge coupling constant exceeds a certain critical value [25]. It is thus plausible that a variety of $4+1$ dimensional gauge theories exhibit confinement at sufficiently large coupling strength.

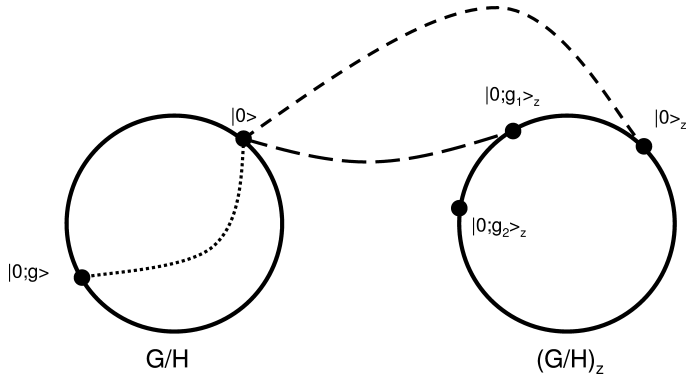

FIG. 1: The vacuum manifold of a $G \otimes Z_2 \to H$ model. The two circles schematically depict the disconnected coset spaces G/H and $(G/H)_z$. Each point along the G/H circle corresponds to a vacuum $|0;g\rangle$ for some $g \in G$, with the corresponding situation for the $(G/H)_z$ circle. The three broken lines represent possible domain wall configurations, with the endpoints at $y = \pm\infty$ on various choices of vacua. The dotted line represents a possible non-topological domain wall configuration. The short-dashed line represents a non clash-of-symmetries domain wall configuration, while the long-dashed line is a clash-of-symmetries domain wall.

domain walls, and explains why the extension to E_6 constructed in Sec.IV is needed. We conclude in Sec.V.

II. THE CLASH OF SYMMETRIES

Consider a theory (an action) whose symmetry group is the direct product of a continuous symmetry group G and a discrete symmetry Z. It is important that Z is *not* a subgroup of G. Suppose the global minima of the Higgs potential spontaneously break G to subgroup H, and simultaneously break Z to a smaller discrete group. For the sake of definiteness, we shall take the $Z = Z_2 = \{1, z \text{ s.t. } z^2 = 1\}$ example in what follows, with the Z_2 completely broken.

The vacuum manifold then consists of two disconnected copies of the coset space G/H, with the copies related by the spontaneously broken $z \in Z_2$. This is an immediate generalisation of the simple Z_2 kink situation, where the vacuum manifold consists of just two disconnected points related by Z_2. Each such point is expanded into the non-trivial manifold G/H. We shall call the disconnected pieces G/H and $(G/H)_z$. The Z_2 must not be a subgroup of G for the two disconnected pieces to exist.

Let $|0\rangle$ be an element of G/H. By definition, $h|0\rangle = |0\rangle$ for all $h \in H$. Since the Higgs potential is G-invariant, if we apply a transformation $g \in G/H$ (that is, a transformation such that $g \in G$ but $g \notin H$) to $|0\rangle$, we obtain a degenerate vacuum state $|0;g\rangle \equiv g|0\rangle$. By considering all possible g's, these transformations generate the G/H piece of the vacuum manifold. Applying the non-identity transformation $z \in Z_2$ from the discrete group, we obtain the discrete image $|0\rangle_z \equiv z|0\rangle$ of $|0\rangle$. This image is a point in the other disconnected piece $(G/H)_z$ of the full vacuum manifold. By applying all possible $g \in G/H$ to $|0\rangle_z$, the space $(G/H)_z$ is generated. Figure 1 illustrates this situation.

The degenerate vacua $|0\rangle$ and $|0;g\rangle$ respect *differently embedded* but otherwise isomorphic subgroups H and H_g, respectively. This is elementary: Let $h_1, h_2 \in H$ such that $h_1 h_2 = h_3 \in H$. Then the conjugates $gh_{1,2,3}g^{-1}$ respect the same multiplication table and hence the set gHg^{-1} is precisely H_g which is isomorphic to H but a different subset of G. If $h|0\rangle = |0\rangle$, then trivially $ghg^{-1}g|0\rangle = g|0\rangle$, which simply says that the conjugated elements preserve the other vacuum: $(ghg^{-1})|0;g\rangle = |0;g\rangle$. Similar statements are true for $(G/H)_z$.

The boundary conditions at $y = \pm\infty$ for domain wall configurations are chosen from the vacua. If the chosen vacua are either both from G/H, or both from $(G/H)_z$, then the "domain wall" configurations are not topologically stable: they are in the same topological class as any of the spatially-homogeneous vacua $|0;g\rangle$, or respectively $|0;g\rangle_z$, and will

dynamically decay to one of these vacua. They may be metastable, depending on the Higgs potential topography,[3] so while they are of some interest we shall not consider them further in this paper.

Topologically non-trivial DW configurations have one boundary condition from G/H and the other from $(G/H)_z$. Evidently, there is an uncountable infinity of such choices, and thus potentially an uncountable infinity of DW solutions, all within the same non-trivial topological class. Figure 1 illustrates the plethora of choices. This potential richness has no analogue for the simple Z_2 kink.

Suppose that the boundary condition at $y = -\infty$ is $|0\rangle$ and at $y = +\infty$ it is $|0\rangle_z$. Then if $h|0\rangle = |0\rangle$, it also follows that

$$h|0\rangle_z \equiv hz|0\rangle = zh|0\rangle = z|0\rangle \equiv |0\rangle_z, \tag{2.1}$$

because by assumption the symmetry is $G \otimes Z$ so that $gz = zg \forall z \in Z, g \in G$ and hence $hz = zh$ always. Thus, the unbroken symmetry at $y = -\infty$ is precisely the same set H as at $y = +\infty$. A domain wall configuration that interpolates between these vacua is then expected to respect the same subgroup H at all y. This is an example of a non-CoS domain wall. Clearly, taking the vacua as any pair $|0; g\rangle$ and $|0; g\rangle_z$ produces a similar outcome (the resulting configuration is nothing more than the g transform of the original one). A non-CoS domain wall is the simplest possible generalisation of a Z_2 kink for a G-invariant theory.

However, there is obviously a second, more interesting possibility: if the vacuum is $|0\rangle$ at $y = -\infty$, then the vacuum at $y = +\infty$ can also be a $|0; g\rangle_z$ for $g \neq 1$. In that case, the subgroups respected asymptotically are the differently-embedded but isomorphic groups H and H_g, respectively. This defines a CoS-style domain wall [14, 15, 16, 17, 18, 19, 20]. At finite y, the configuration would be expected to respect the smaller group $H \cap H_g$ due to the fact that the solution has to "reconcile" boundary conditions that have different stability groups that "clash".[4]

So, there will be an infinite family of non-CoS DWs, trivially related to each other by global transformations $g \in G/H$. They all have the same energy density, because the Hamiltonian is invariant under G. The CoS DWs have a more complicated spectrum. Consider two configurations, $\chi_1(y)$ and $\chi_2(y)$, with χ_1 interpolating between $|0\rangle$ and $|0; g_1\rangle_z$, while χ_2 interpolates between $|0\rangle$ and $|0; g_2\rangle_z$, such that $g_1 \neq g_2$. Suppose, for the moment, that G is a global but not a local symmetry. These two solutions *cannot* be transformed into each by a *global* G-transformation, so they would be expected to have different energy densities (their configurations trace different paths through the Higgs potential topography). As a corollary, the non-CoS solutions should have a different energy density from the CoS solutions. All these solutions are in the same topological class, so finite-energy dynamical evolution between them is allowed. Hence, the special configurations within that topological class that minimise the energy density will be topologically stable. The others should be unstable to decay to the minimum-energy configurations, which play the role of "vacua" for the "kink-sector". This general reasoning cannot tell you which configuration has the minimum energy-density: you need to calculate that within a specific model. For example, in the toy model considered in Ref. [14] the sign of a Higgs potential parameter determined whether the non-CoS or a CoS solution was energetically favoured.

Suppose now that G is a gauge symmetry, and again consider the configurations discussed in the previous paragraph, together with the specification of vanishing gauge fields A_M at the solution-level. The non-CoS solutions remain connected through global transformations. Two CoS scalar field configurations, χ_1 and χ_2, can be written as local G-transforms of each other. Suppose that

$$\chi_2(y) = U(y)\chi_1(y), \tag{2.2}$$

where $U(y)$ is a local-G element. Then the original first solution

$$\chi = \chi_1(y), \qquad A_M = 0 \tag{2.3}$$

---

[3] We dread to use the term "landscape".

[4] From experience, we have found that $H \cap H_g$ is the usual outcome. The specifics depend on the case considered. Sometimes there is enhanced symmetry at $y = 0$ because some of the scalar multiplet components instantaneously vanish there. This enhancement on a set of measure zero has yet to find application, although speculations exist [17, 30].

is gauge-equivalent to

$$\chi = \chi_2(y), \qquad A_M = -\frac{i}{e}(\partial_M U)U^\dagger, \tag{2.4}$$

where e is the gauge coupling constant, but it is *not* gauge-equivalent to

$$\chi = \chi_2(y), \qquad A_M = 0, \tag{2.5}$$

which is the original second solution. Thus the two solutions $\chi = \chi_1,\ A_M = 0$ and $\chi = \chi_2,\ A_M = 0$ have different energy densities, even though the scalar-field portions are related by a local symmetry transformation. Although $A_M = -\frac{i}{e}(\partial_M U)U^\dagger$ is a pure-gauge configuration, it contributes to the energy density through the $\chi - A_M$ interaction terms.

Setting the gauge fields to zero at the solution-level is basically a convenient choice of gauge, one we shall adopt from now on. Of course the solutions can be made to look very different by gauge-transforming them, but their physical consequences cannot change. This circumstance is no different from the monopole or local-string cases, where again the solutions look different in different gauges. Actually, it is no more complicated than the usual homogeneous vacuum expectation value (VEV) case. If $\langle\chi\rangle$ is a homogeneous VEV, then it can be gauge-transformed to a non-homogeneous configuration $U(x)\langle\chi\rangle$ but the scalar gradient energy is cancelled by the gauge-field contribution.

The alert reader may have noticed the following: we have not proven that the minimum-energy DW configuration must have a gauge-field sector that is gauge-equivalent to zero. This does indeed appear to be a loose end. We shall make the assumption that it is in fact true for the purposes of the rest of this paper. Ultimately, one could uncover its hypothetical falsity by a perturbative stability analysis for the DW, but that is well beyond the scope of the present investigation.

Finally, a technical point: The set of H_g contains an uncountable infinity of differently-embedded but isomorphic subgroups. However, there is a certain useful sense in which the number of embeddings can be considered finite. Let the Cartan subalgebra $\mathcal{G}_C$ of G be a certain particular set of generators, corresponding to a particular choice of basis for the Lie algebra. If we require that the Cartan subalgebras of two subgroups H_{g_1} and H_{g_2} are both subspaces of $\mathcal{G}_C$, then the number of distinct embeddings is finite. A familiar example of this concerns the $SU(2)$ subgroups of $SU(3)$. While there are an uncountable infinity of ways of embedding $SU(2)$ in $SU(3)$, there are only three embeddings that have the $SU(2)$ Cartan subalgebras as subspaces of the given Cartan-subalgebra space of $SU(3)$. These are usually called I-spin, U-spin and V-spin. When we say "different embeddings" below, this is what we shall mean.[5]

III. $SO(10)$ WARM-UP EXAMPLE: THE NEED FOR E_6

We now discuss a $G = SO(10)$ model that serves both as a warm-up for E_6 and explains why the extension to E_6 is necessary. We shall make use of the $O(10)$-kink analysis of Ref. [17]. While some recapitulation is necessary for completeness, we shall be as brief as possible, and the reader is referred to Ref. [17] for a detailed discussion.

Let χ be a scalar multiplet in the adjoint representation, the 45, of $SO(10)$. The most general quartic Higgs potential is

$$V = \frac{1}{2}\,\mu^2\,\mathrm{Tr}(\chi^2) + \frac{1}{4}\,\lambda_1\,\mathrm{Tr}(\chi^2)^2 + \frac{1}{4}\,\lambda_2\,\mathrm{Tr}(\chi^4), \tag{3.1}$$

where $\chi = f_\alpha \hat{X}^\alpha$ with the $\hat{X}$'s being matrix representations of the generators in the fundamental of $SO(10)$ while the f_α's are the components of the adjoint multiplet. The matrix χ is antisymmetric and transforms as per $\chi \to A\chi A^T$

[5] Note that taking linear combinations of Cartan generators to define different embeddings is in accord with Dynkin's general theory of embeddings [31]. In that formalism, the embedding of an algebra $\mathcal{H}$ into a simple or semi-simple algebra $\mathcal{G}$ is fully defined by a mapping F from the Cartan subalgebra of $\mathcal{H}$ into the Cartan subalgebra of $\mathcal{G}$, as per $H_\alpha \to F(H_\alpha) = \sum_{a=1}^{n} F_{\alpha a} G_a$, where H_α $(\alpha = 1, 2, \ldots, m)$ and G_a $(a = 1, 2, \ldots, n)$ are the Cartan generators of $\mathcal{H}$ and $\mathcal{G}$, respectively. The matrix $(F_{\alpha a})$ is the defining matrix of the embedding, and two embeddings are different if their defining matrices are different.

where A is an $SO(10)$ fundamental-representation matrix. The parameter μ^2 is chosen to be positive since $\mathrm{Tr}(\chi^2)$ is negative definite. The cubic invariant $\mathrm{Tr}(\chi^3)$ identically vanishes so there is an accidental discrete Z_2 symmetry, $\chi \to -\chi$, which shall play the role of Z. It is not a subgroup of $O(10)$.

The global minimisation of such a potential was performed by Li [32] (see also [33]). Using an $SO(10)$ transformation, one may always bring a VEV pattern into the standard form

$$\chi = \mathrm{diag}(f_1\,\epsilon\,,\, f_2\,\epsilon\,,\, f_3\,\epsilon\,,\, f_4\,\epsilon\,,\, f_5\,\epsilon), \tag{3.2}$$

where the f_i are real and

$$\epsilon \equiv i\,\sigma_2 = \begin{pmatrix} 0 & 1 \\ -1 & 0 \end{pmatrix}. \tag{3.3}$$

The five independent fields f_i correspond to the five generators in the $SO(10)$ Cartan subalgebra. In this basis,

$$V = -\mu^2 \sum_{i=1}^{5} f_i^2 + \lambda_1 \left(\sum_{i=1}^{5} f_i^2\right)^2 + \frac{1}{2}\,\lambda_2 \sum_{i=1}^{5} f_i^4. \tag{3.4}$$

For $\lambda_2 > 0$, the global minima of V are at

$$f_i^2 = \frac{\mu^2}{10\lambda_1 + \lambda_2} \quad \equiv f_{\min}^2 \ \forall i, \tag{3.5}$$

where we define $f_{\min} \equiv \sqrt{\mu^2/(10\lambda_1 + \lambda_2)}$ and the unbroken subgroup is $H = U(5)$. The values of f_i at the minima are specified up to a sign that can be chosen independently for each component

$$f_i = \pm f_{\min}. \tag{3.6}$$

Different choices for these signs correspond to two features: different embeddings of $U(5)$ in $SO(10)$ and also a choice of which Z_2 sector the minimum lies in.

To explore this further, let us turn to possible domain wall configurations. Suppose that at $y = -\infty$, we choose as our boundary condition

$$\chi(-\infty) = -f_{\min}^{(5)} \equiv -f_{\min}\,\mathrm{diag}(\epsilon\,,\,\epsilon\,,\,\epsilon\,,\,\epsilon\,,\,\epsilon). \tag{3.7}$$

This defines a certain $U(5)$ unbroken at $y = -\infty$, and the VEV lies in one of the two disconnected pieces of the vacuum manifold. At $y = +\infty$, there are three choices that lie in the other piece of the vacuum manifold, disconnected from the first by the spontaneously broken Z_2:

$$\chi(+\infty) = \begin{cases} f_{\min}^{(5)} & \equiv \quad f_{\min}\,\mathrm{diag}(\epsilon\,,\,\epsilon\,,\,\epsilon\,,\,\epsilon\,,\,\epsilon) \\ f_{\min}^{(3,2)} & \equiv \quad f_{\min}\,\mathrm{diag}(\epsilon\,,\,\epsilon\,,\,\epsilon\,,\,-\epsilon\,,\,-\epsilon) \\ f_{\min}^{(4,1)} & \equiv f_{\min}\,\mathrm{diag}(\epsilon\,,\,-\epsilon\,,\,-\epsilon\,,\,-\epsilon\,,\,-\epsilon) \end{cases}. \tag{3.8}$$

(Permutations of the minus signs in the last two of these vacua are just a trivial rearrangement of the representation-space and need not be separately considered.) Vacua with an odd number of minus signs on the right-hand side on Eq. (3.8) are continuously connected to $\chi(-\infty)$ by $SO(10)$ and shall not be considered as they would give rise to non-topological domain walls.

The three vacua in Eq. (3.8) are invariant under differently-embedded subgroups of $SO(10)$: $U(5)_1$, $U(5)_2$ and $U(5)_3$. The superscripts (5), $(3,2)$ and $(4,1)$ denote the numbers of plus and minus signs in the VEVs. But they also usefully describe the unbroken symmetry of the domain wall at finite y, respectively

$$U(5), \qquad U(3) \otimes U(2) \quad \text{and} \qquad U(4) \otimes U(1), \tag{3.9}$$

as we now explain.

The ansatz for domain wall configurations that interpolate between the stated boundary conditions is $\chi(y) = h(y)\chi(-\infty)+g(y)\chi(+\infty)$, where the functions h and g obey self-evident boundary conditions. The first configuration, which interpolates between $-f_{\rm min}$ and $+f_{\rm min}$ for all components $f_i(y)$, breaks $SO(10)$ to $U(5)_1$ at all values of y, because the relative magnitudes of the components are always the same at a given y. It is a non-CoS domain wall. The second configuration has an equal-magnitude 3×3 block (of 2×2 submatrices), and an equal-magnitude 2×2 block. The unbroken symmetry is then

$$U(3)\otimes U(2) = U(5)_1 \cap U(5)_2. \tag{3.10}$$

Similarly, the third configuration's block structure leads to $U(4)\otimes U(1) = U(5)_1 \cap U(5)_3$.

The Euler-Lagrange equations

$$f_i'' = 2\left[-\mu^2 + 2\lambda_1 \sum_{j=1}^{5} f_j^2\right] f_i + 2\lambda_2 f_i^3, \tag{3.11}$$

with the three types of boundary conditions above may be solved numerically. However, a simple way to prove that solutions exist is to consider the $\lambda_1 = 0$ slice through parameter space. The equations can then be solved analytically to yield

$$f_i(y) = f_{\rm min}\tanh(\mu y)\ \forall i \tag{3.12}$$

for the first boundary condition choice,

$$f_i(y) = f_{\rm min}\tanh(\mu y) \text{ for } i = 1,2,3 \text{ and } f_i(y) = f_{\rm min} \text{ for } i = 4,5 \tag{3.13}$$

for the second choice, and

$$f_i(y) = f_{\rm min}\tanh(\mu y) \text{ for } i = 1 \text{ and } f_i(y) = f_{\rm min} \text{ for } i = 2,3,4,5 \tag{3.14}$$

for the third choice. The surface energy densities are in the ratios $5:3:1$ for the first to the third solutions [17], so Eq. (3.14) gives the topologically stable configuration.

From a Dvali-Shifman point of view, this stable configuration has an unbroken $SU(4)$ on the brane that is embedded in $SU(5)_1$ on the $y<0$ side of the wall, and $SU(5)_3$ on the $y>0$ side. The $SU(4)$ gauge bosons are thus localised to the wall, if the Dvali-Shifman mechanism is correct, because by assumption both $SU(5)_1$ and $SU(5)_3$ are in confinement phase in their respective bulk regions. This establishes the connection between clash-of-symmetries and Dvali-Shifman by way of an explicit rigorously worked-out solution. It is, however, just a toy model since the symmetry breaking pattern is not what is required phenomenologically.

The second configuration, with

$$U(3)\otimes U(2) = SU(3)\otimes SU(2)\otimes U(1)\otimes U(1) \tag{3.15}$$

on the brane is closer to what we need for a realistic model. While the analytic solution of Eq. (3.13) is unstable to dynamical evolution to Eq. (3.14), it could well be that in another region of Higgs-potential parameter space the $U(3)\otimes U(2)$ solution is the stable one. This has not been established, but let us suppose it is true. The model then still does not quite work, although it comes close.

It is certainly true that the $SU(3)\otimes SU(2)$ factor in Eq. (3.15) is Dvali-Shifman-localised, because it is a subgroup of both $SU(5)_1$ (the bulk symmetry for $y<0$) and $SU(5)_2$ (the bulk symmetry for $y>0$). However, there is a problem with the hypercharge gauge boson corresponding to $U(1)_Y$. To see this, we need to examine the $U(1)$ generators more closely.

The asymptotic gauge groups are

$$U(5)_1 = SU(5)_1\otimes U(1)_{X_1} \qquad \text{and} \qquad U(5)_2 = SU(5)_2\otimes U(1)_{X_2}. \tag{3.16}$$

Denote by Y_1 the hypercharge generator inside $SU(5)_1$, and Y_2 the one inside $SU(5)_2$. The two $U(1)$'s in Eq.(3.15) can be taken to be generated either by Y_1 and X_1, or by Y_2 and X_2, and each pair can be written as linear combinations of the other pair. Now, either Y_1 or Y_2 can be the physical hypercharge Y. Which one is selected will be an accident of spontaneous symmetry breaking. At some scale above the electroweak, the breaking

$$U(1)_{Y_1} \otimes U(1)_{X_1} = U(1)_{Y_2} \otimes U(1)_{X_2} \to U(1)_Y, \tag{3.17}$$

with either $Y = Y_1$ or $Y = Y_2$, will have to take place to produce an effective standard model at low-energies (this will require an additional Higgs field). Suppose $Y = Y_1$ is spontaneously selected. Then the hypercharge gauge boson cannot propagate into the $y < 0$ bulk, but a component of it will propagate into the $y > 0$ bulk. The generator $Y = Y_1$ is a linear combination of Y_2 and X_2, so the hypercharge gauge field is a linear combination of the gauge fields of Y_2 and X_2. But only the Y_2 part is unable to propagate into the $y > 0$ region; the X_2 part is immune from the Dvali-Shifman effect because it is not confining. After electroweak symmetry breaking, this will imply that both the photon and Z^0 will leak into the $y > 0$ bulk, which is phenomenologically ruled out. If Y_2 happens to become the physical Y, then leakage into $y < 0$ will occur.

This structure, with localised gluons and $W^\pm$ bosons, but semi-delocalised photons and Z^0's, almost works. But understanding its pathology also provides the cure: We need to expand the symmetry on the brane to contain a full $SU(5)$, with the physical hypercharge identified with one of its generators. Further, this brane-$SU(5)$ must be a subgroup of confining non-Abelian groups on both sides of the domain wall. These two features automatically arise when we upgrade from $SO(10)$ to E_6 as the symmetry of the action.

IV. THE E_6 DOMAIN-WALL BRANE.

A. Group theory

Take a scalar field multiplet χ in the 78-dimensional adjoint representation of E_6. In the next subsection, we shall analyse the associated Higgs potential and produce domain wall solutions. But for now, we just need to use the fact that for a range of parameters the global minima of the potential will induce

$$E_6 \to SO(10) \otimes U(1), \tag{4.1}$$

which is a maximal subgroup. Now consider different embeddings of $SO(10) \otimes U(1)$ in E_6.[6] We shall show below that there is a pair of embeddings, which we shall call simply $SO(10) \otimes U(1)_E$ and $SO(10)' \otimes U(1)_{E'}$, that is of particular interest for model-building.[7] The domain wall solution we shall find in the next subsection interpolates between χ VEVs that break E_6 to these different but isomorphic subgroups on opposite sides of the wall. The symmetry on the wall is then

$$[\, SO(10) \otimes U(1)_E \,] \cap [\, SO(10)' \otimes U(1)_{E'} \,] = SU(5) \otimes U(1)_E \otimes U(1)_{E'}, \tag{4.2}$$

as we shall establish. Since $SU(5) \subset SO(10) \cap SO(10)'$, the Dvali-Shifman mechanism localises all the $SU(5)$ gauge bosons to the domain wall, including the photon and the Z^0.

Let us look at the group theory in more detail. Under

$$E_6 \to SO(10) \otimes U(1)_E \to [\, SU(5) \otimes U(1)_X \,] \otimes U(1)_E, \tag{4.3}$$

the fundamental 27-dimensional representation of E_6 branches as per

$$\begin{aligned} 27 \;&\to\; 1(4) + 10(-2) + 16(1) \\ &\to\; 1^{(0,4)} + [\, 5^{(2,-2)} + 5^{*(-2,-2)} \,] + [\, 1^{(-5,1)} + 5^{*(3,1)} + 10^{(-1,1)} \,]. \end{aligned} \tag{4.4}$$

---

[6] We mean the finite number of embeddings in the sense of the final paragraph of Sec. II.
[7] The second embedding has been used in unified model building [34, 35, 36, 37].

The notation for $SO(10)\otimes U(1)_E$ representations is $D(12E)$, where D is the dimension of the $SO(10)$ multiplet, and the $U(1)_E$ generator has been normalised as per

$$\mathrm{Tr}_{27}(E^2)=\frac{1}{2}. \tag{4.5}$$

(We use $12E$ to make the charges integers for convenience.) The $SU(5)\otimes U(1)_X\otimes U(1)_E$ notation is $D^{(4\sqrt{15}X,12E)}$ with

$$\mathrm{Tr}_{27}(X^2)=\frac{1}{2},\qquad \mathrm{Tr}_{27}(EX)=0. \tag{4.6}$$

The second embedding is revealed by considering the linear combinations

$$X'=-\frac{1}{4}(X+\sqrt{15}E),\qquad E'=\frac{1}{4}(-\sqrt{15}X+E) \tag{4.7}$$

that correspond to

$$E_6\to SO(10)'\otimes U(1)_{E'}\to [\,SU(5)\otimes U(1)_{X'}\,]\otimes U(1)_{E'}. \tag{4.8}$$

Rewriting the multiplets from $D^{(4\sqrt{15}X,12E)}$ notation to $D_{(4\sqrt{15}X',12E')}$ notation, we see that

$$\begin{aligned}
1^{(0,4)} &= 1_{(-5,1)}\\
5^{(2,-2)} &= 5_{(2,-2)}\\
5^{*(-2,-2)} &= 5^*_{(3,1)}\\
1^{(-5,1)} &= 1_{(0,4)}\\
5^{*(3,1)} &= 5^*_{(-2,-2)},\\
10^{(-1,1)} &= 10_{(-1,1)},
\end{aligned} \tag{4.9}$$

so the 5^*'s flip roles as do the singlets. Let us now redundantly denote the multiplets through

$$D^{(4\sqrt{15}X,12E)}_{(4\sqrt{15}X',12E')}. \tag{4.10}$$

The 10 of $SO(10)'$ is

$$5^{(2,-2)}_{(2,-2)}\oplus 5^{*(3,1)}_{(-2.-2)}, \tag{4.11}$$

whereas the 10 of the original $SO(10)$ was instead formed by

$$5^{(2,-2)}_{(2,-2)}\oplus 5^{*(-2,-2)}_{(3,1)}. \tag{4.12}$$

Similarly, the 16 of $SO(10)'$ consists of

$$1^{(0,4)}_{(-5,1)}\oplus 5^{*(-2,-2)}_{(3,1)}\oplus 10^{(-1,1)}_{(-1,1)}, \tag{4.13}$$

whereas the 16 of the original $SO(10)$ consisted of

$$1^{(-5,1)}_{(0,4)}\oplus 5^{*(3,1)}_{(-2,-2)}\oplus 10^{(-1,1)}_{(-1,1)}. \tag{4.14}$$

The $SO(10)'$ singlet is $1^{(-5,1)}_{(0,4)}$, whereas the original $SO(10)$ singlet is $1^{(0,4)}_{(-5,1)}$.

Because all higher-dimensional representations of E_6 are formed from products of 27's, the feature that some $SU(5)\otimes U(1)^2$ submultiplets flip when $(X,E)\to(X',E')$ propagates to all irreducible E_6 representations. The submultiplets can be packaged in $SO(10)\otimes U(1)_E$ multiplets, or repackaged into $SO(10)'\otimes U(1)_{E'}$ multiplets. This

establishes, constructively, that the two embeddings exist, and that Eq. (4.2) is true.[8] Note that the additional $U(1)$'s are there because adjoint configurations cannot rank-reduce.

Let us repeat this exercise for the adjoint of E_6:

$$\begin{aligned} 78 \;&\to\; 1(0) + 45(0) + 16(-3) + 16^*(3) \qquad (4.15)\\ &\to\; 1^{(0,0)}_{(0,0)} \\ &+\; [\,1^{(0,0)}_{(0,0)} + 10^{(4,0)}_{(-1,-3)} + 10^{*(-4,0)}_{(1,3)} + 24^{(0,0)}_{(0,0)}\,] \\ &+\; [\,1^{(-5,-3)}_{(5,3)} + 5^{*(3,-3)}_{(3,-3)} + 10^{(-1,-3)}_{(4,0)}\,] \\ &+\; [\,1^{(5,3)}_{(-5,-3)} + 5^{(-3,3)}_{(-3,3)} + 10^{*(1,3)}_{(-4,0)}\,] \qquad (4.16) \end{aligned}$$

The flipping of roles is evidently

$$\begin{aligned} 1^{(0,0)}_{(0,0)} \;&\leftrightarrow\; 1^{(0,0)}_{(0,0)}, \\ 10^{*(-4,0)}_{(1,3)} \;&\leftrightarrow\; 10^{*(1,3)}_{(-4,0)}, \\ 10^{(4,0)}_{(-1,-3)} \;&\leftrightarrow\; 10^{(-1,-3)}_{(4,0)}, \\ 1^{(-5,-3)}_{(5,3)} \;&\leftrightarrow\; 1^{(5,3)}_{(-5,-3)}. \end{aligned} \qquad (4.17)$$

The $SU(5)$ adjoint $24^{(0,0)}_{(0,0)}$ is common to both $SO(10)$ embeddings, as befits its status of being in the intersection of the two.

The two $1^{(0,0)}_{(0,0)}$ multiplets play important roles. Giving a VEV to the $1(0)$ in Eq. (4.15) breaks E_6 to $SO(10)\otimes U(1)_E$, while a VEV for the second singlet in Eq. (4.16) breaks E_6 to $SO(10)'\otimes U(1)_{E'}$. A clash-of-symmetries kink interpolates between these two VEVs imposed as boundary conditions. At $|y| < \infty$, both $SU(5)\otimes U(1)^2$ singlet components of the 78 have nonzero values, and this is precisely why the configuration breaks E_6 to the intersection of the two subgroups. To analyse this further, we must consider the dynamics.

B. Higgs potential and domain-wall solutions

The adjoint scalar multiplet χ shall be represented by

$$\chi = f_\alpha \hat{X}^\alpha, \quad \alpha = 1, \ldots, 78 \qquad (4.18)$$

where $\hat{X}$'s are matrix representations of the generators for the 27 of E_6, and the f's are the field components. It transforms according to

$$\chi \to U\chi U^\dagger \qquad (4.19)$$

where U is group representation matrix for the 27. We shall only be concerned with two of the seventy-eight fields: those associated with (E, E'), equivalently (X, E) or (X', E') depending on what basis we choose for the Lie algebra.

We thus specialise to

$$\chi = f_E E + f_X X \equiv \tilde{f}_E E + f_{E'} E' \qquad (4.20)$$

with

$$\tilde{f}_E \equiv f_E + \frac{f_X}{\sqrt{15}}, \qquad f_{E'} \equiv -\frac{4 f_X}{\sqrt{15}}, \qquad (4.21)$$

---

[8] By considering additional Cartan generators beyond E and X, more embeddings of $SO(10)$ can be found. This is discussed further in the appendix.

according to Eq. (4.7). The (X, E) basis is the more convenient for solving the Euler-Lagrange equations, because E and X are orthogonal as per Eq. (4.6). The (E, E') basis, however, is the simplest one for thinking about the two embeddings.

The VEVs we want for the boundary conditions are

$$(\tilde{f}_E, f_{E'}) = v(1, 0), \tag{4.22}$$

which corresponds to $E_6 \to SO(10) \otimes U(1)_E$. The other VEV is

$$(\tilde{f}_E, f_{E'}) = -v(0, 1) \tag{4.23}$$

which gives $E_6 \to SO(10)' \otimes U(1)_{E'}$. The relative minus sign between Eqs. (4.22) and (4.23) comes from the breaking of a

$$\chi \to -\chi \tag{4.24}$$

discrete symmetry we shall impose on the Higgs potential, and it is *crucial* for two reasons. First, the spontaneous Z_2 breaking will ensure that our domain walls are topologically non-trivial. Second, it leads to a remarkable outcome for fermion zero-mode localisation, to be explained in the next subsection.

In terms of the (X, E) basis, these same VEVs are

$$(f_X, f_E) = v(0, 1) \quad \text{and} \quad v\left(\frac{\sqrt{15}}{4}, -\frac{1}{4}\right), \tag{4.25}$$

respectively.

We now need to find a Higgs potential with these two VEVs as degenerate global minima. The Higgs potential is constructed out of adjoint invariants, which according to Eqs. (4.19) and (4.18) are

$$I_n = \mathrm{Tr}(\chi^n) = \mathrm{Tr}(\hat{X}^{\alpha_1}\hat{X}^{\alpha_2}\cdots\hat{X}^{\alpha_n})f_{\alpha_1}f_{\alpha_2}\cdots f_{\alpha_n}. \tag{4.26}$$

They are simply the nth order Casimir invariants. According to Refs. [38, 39], the independent invariants are

$$I_2,\ I_5,\ I_6,\ I_8,\ I_9,\ I_{12}, \tag{4.27}$$

which immediately has an interesting consequence: the fact that $I_{5,9}$ are nonzero means that the discrete Z_2 of Eq.(4.24) is *not a subgroup* of E_6, because imposing it eliminates the otherwise present odd-power invariants.

It is sensible to truncate the Higgs potential at order-six:

$$V = -\lambda_1 I_2 + \lambda_2 (I_2)^2 - 2304\kappa I_6 + \frac{4}{3}\lambda_3 (I_2)^3 \tag{4.28}$$

where some peculiar numbers and signs have been inserted for later convenience. In the extra-dimensional setting, field-theoretic models must generally be considered as effective theories valid below an ultraviolet cutoff scale Λ, because they are almost inevitably non-renormalisable. In writing down a Higgs potential, one simply adds terms of ever higher mass-dimension and truncates appropriately, given that the higher the mass-dimension the more suppressed it should become. For the E_6 application, it is not helpful to truncate at fourth order, because the only fourth-order invariant is $(I_2)^2$ and I_2 is invariant under an accidental $O(78)$ symmetry. The presence of I_6 reduces the symmetry of the Higgs potential to E_6 (presumably), and eliminates a pseudo-Goldstone boson issue.[9]

Equation (4.28) is a complicated sextic in seventy-eight fields. But to perform the global minimisation analysis, one can always transform any VEV pattern to a standard form given by linear combinations of just the six generators

[9] An alternative is to truncate the classical theory at fourth order, but to add a Coleman-Weinberg potential generated through quantum corrections that explicitly break the $O(78)$ [39].

in the Cartan subalgebra of E_6. This produces a still quite complicated sextic in six fields. To make our discussion as simple as possible, in the main body of the paper we shall further truncate to just the two Cartan subalgebra generators of interest, and use Eq. (4.20). We extend the global minimisation analysis to all six fields in the appendix.

With just $f_{E,X} \neq 0$, the nth-order invariant simplifies to

$$I_n = \sum_{k=0}^{n} \begin{pmatrix} n \\ n-k \end{pmatrix} \mathrm{Tr}(E^{n-k} X^k) f_E^{n-k} f_X^k. \tag{4.29}$$

The traces can be worked out by hand, because we know the matrix representations of E and X from the branching rules in Eq. (4.4). We obtain

$$I_2 = \frac{1}{2}(f_E^2 + f_X^2), \tag{4.30}$$

$$I_6 = \frac{1}{2304}\left(f_E^6 + 5 f_E^4 f_X^2 + 7 f_E^2 f_X^4 - \frac{48}{5\sqrt{15}} f_E f_X^5 + \frac{83}{25} f_X^6 \right). \tag{4.31}$$

To understand the extrema of Eq. (4.28), it is helpful to use the polar decomposition

$$f_E = r\cos\theta, \qquad f_X = r\sin\theta. \tag{4.32}$$

The VEVs of Eq. (4.25) are then

$$(10,+) \ : \qquad \theta = 0, \tag{4.33}$$

$$(10',-) \ : \qquad \cos\theta = -\frac{1}{4}, \ \sin\theta = \frac{\sqrt{15}}{4}. \tag{4.34}$$

The notation $(10,+)$ means that the VEV of Eq. (4.33) induces $E_6 \to SO(10) \otimes U(1)_E$, and we have (arbitrarily) assigned it a positive Z_2 "parity" which signals that it lies in G/H rather than $(G/H)_z$. Similarly, $(10',-)$ means $E_6 \to SO(10)' \otimes U(1)_{E'}$ and it lies in $(G/H)_z$. There is another pair, with the opposite Z_2 parities:

$$(10,-) \ : \qquad \theta = \pi, \tag{4.35}$$

$$(10',+) \ : \qquad \cos\theta = \frac{1}{4}, \ \sin\theta = -\frac{\sqrt{15}}{4}. \tag{4.36}$$

The topological CoS domain wall connects $(10,+)$ and $(10',-)$, accompanied by a CoS anti-domain-wall connecting $(10,-)$ and $(10',+)$. The topological non-CoS domain walls connect $(10,+)$ with $(10,-)$ [breaking E_6 to $SO(10) \otimes U(1)_E$ at all y], and $(10',+)$ with $(10',-)$ [breaking E_6 to $SO(10)' \otimes U(1)_{E'}$ at all y]. There are also nontopological configurations: (i) $(10,+)$ connected to $(10',+)$, and (ii) $(10,-)$ connected to $(10',+)$, which are both CoS-like.

Figure 2 display the invariants $-I_6/r^6$, $-I_8/r^8$, $-(I_5)^2/r^{10}$ and $-I_{12}/r^{12}$ as functions of θ. They show a remarkably similar structure. It is evident that the global minima for all four invariants are precisely the four VEVs of Eqs. (4.33-4.36). It is clear from this that choosing to truncate at the sextic level, as in Eq. (4.28), does not sacrifice much in terms of generality. We can be confident that our simplified potential leads to solutions whose qualitative characteristics would be retained were a wider class of higher-order potentials considered. In addition, the appendix shows that there are no deeper minima than $(10,\pm)$ and $(10',\pm)$ in the whole six-dimensional Cartan domain.

The sign in front of I_6 must be negative to achieve the desired extrema as minima rather than maxima. The other terms in the Higgs potential, Eq. (4.28), are independent of θ, depending only on the radial function r. Hence, it is clear that Eq. (4.28) has the global minima we require. Figure 3 shows a contour plot of the Higgs potential for a certain parameter choice illustrating this conclusion. It is important to realise that although the minima $(10,+)$ and $(10',+)$ [similarly $(10,-)$ and $(10',-)$] look as though they are disconnected by E_6, this is just an illusion created by only plotting the two-dimensional (f_X, f_E) slice through the 78-dimensional adjoint representation space. Minima with opposite parities are definitely disconnected from each other.[10]

---

[10] While it is certainly true that the Z_2 is not a subgroup of E_6, so that in general χ and $-\chi$ are disconnected from each other, one may

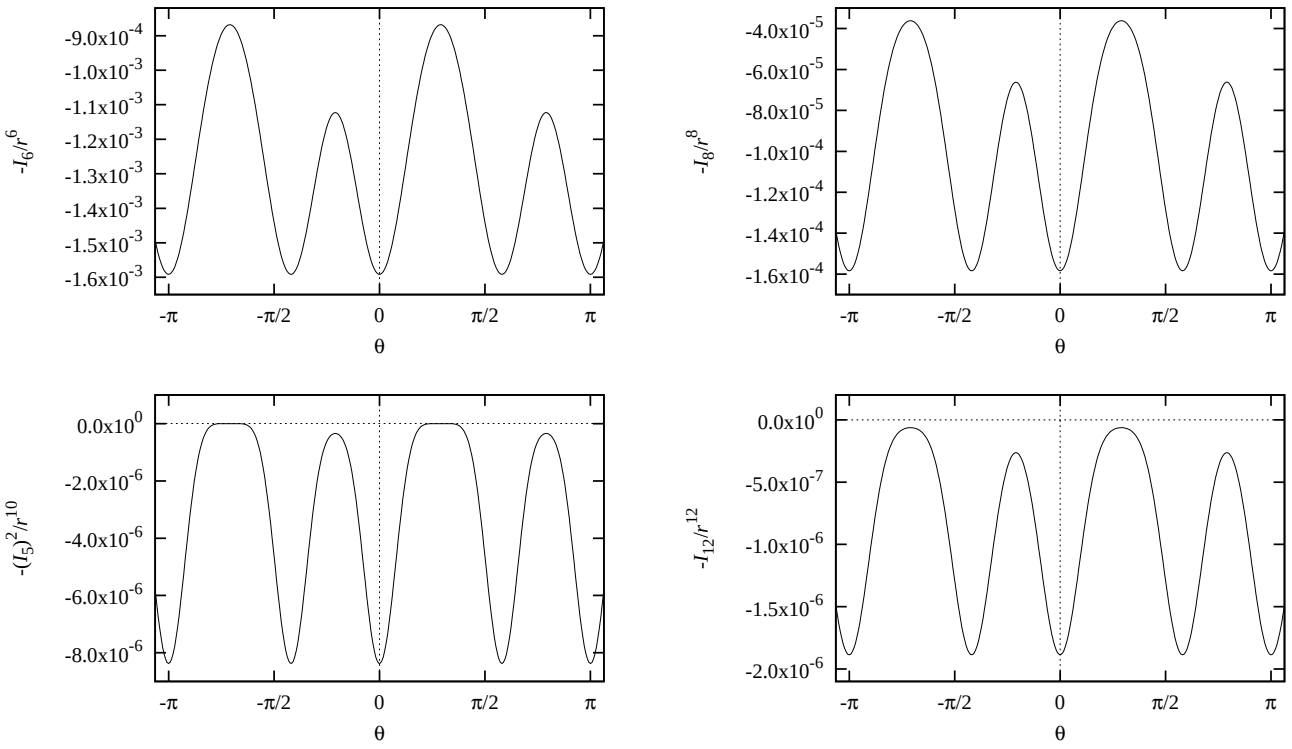

FIG. 2: The invariants $-I_6/r^6$, $-I_8/r^8$, $-(I_5)^2/r^{10}$ and $-I_{12}/r^{12}$ as functions of θ. Note the remarkable similarity. The global minima for all four, reading from left to right, are: $(10,-)$, $(10',+)$, $(10,+)$, $(10',-)$ and then $(10,-)$ again (see text for explanation of this notation).

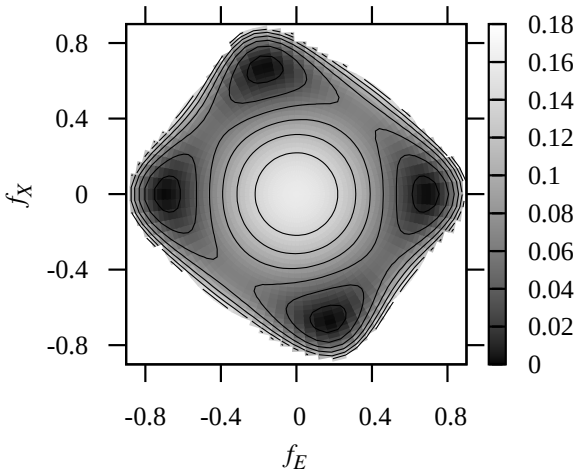

FIG. 3: Contour plot of the Higgs potential as a function of the two field components f_E and f_X. The parameters used are $\kappa = 0.8$, $\lambda_1 = 1.0$, $\lambda_2 = 0$, $\lambda_3 = 22.0$. The darkest regions are the global minima in the order $(10,+)$, $(10',-)$, $(10,-)$ and $(10',+)$ reading anticlockwise from the rightmost minimum. The light area near the origin is a local maximum.

worry that there is nevertheless an E_6 transformation that takes the specific configuration $(10,+)$ to $(10,-)$. However, this is not the case. Explicit calculation of the E_6 invariant I_5 reveals a nonzero f_E^5 term. Hence, $f_E \to -f_E$ must be outside of E_6. It does not matter that I_5 has been omitted from the Higgs potential, as it is a purely group-theoretic argument.

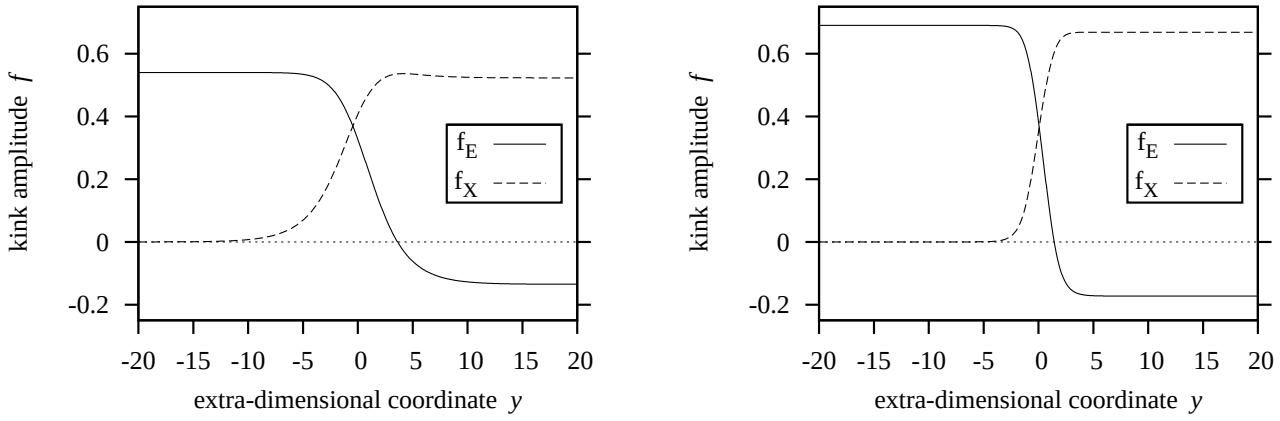

FIG. 4: Clash-of-symmetries domain wall solutions interpolating between $(10,+)$ at $y=-\infty$ and $(10',-)$ at $y=+\infty$. The parameters used in the left plot are $\kappa=0.2$, $\lambda_1=1.5$, $\lambda_2=0$, $\lambda_3=22.0$; those in the right plot are $\kappa=0.8$, $\lambda_1=1.0$, $\lambda_2=0$, $\lambda_3=22.0$.

In the examples presented below, we further simplify the Higgs potential by setting $\lambda_2=0$ as this term does not play an important role. It is then easy to show that at the degenerate minima,

$$r=v\equiv\left(\frac{\lambda_1}{\lambda_3-22\kappa}\right)^{1/4}, \tag{4.37}$$

so we must take $\lambda_3>22\kappa$, and that the value of V at the minima is

$$V_{\min}=-\frac{1}{3}\sqrt{\frac{\lambda_1^3}{\lambda_3-22\kappa}}. \tag{4.38}$$

The latter must be subtracted from the potential

$$V\to V-V_{\min} \tag{4.39}$$

to produce finite energy-densities for the domain wall configurations. Figure 3 is a contour plot of the potential energy showing the four degenerate global minima.

Having understood the global minima, we may now solve the Euler-Lagrange equations

$$f_X''(y)=\frac{\partial V}{\partial f_X},\qquad f_E''(y)=\frac{\partial V}{\partial f_E} \tag{4.40}$$

using those VEVs as boundary conditions. Numerical solutions for CoS domain walls interpolating between $(10,+)$ at $y=-\infty$ and $(10',-)$ at $y=+\infty$ with two different parameter choices are displayed in Figure 4.

Figure 5 depicts non-CoS domain wall solutions for the same parameter choices. The function f_X is zero, while f_E interpolates between v and $-v$ in archetypal kink fashion. This means that the non-CoS configurations feel the large potential-energy maximum at $f_X=f_E=0$, while the CoS configuration "skirts around" that central maximum. This immediately implies that the CoS solutions have lower energy density than the non-CoS solutions. Although they are in the same topological class, the CoS domain walls are stable while the non-CoS domain walls are unstable. Figure 6 shows a three-dimensional plot of the potential and where the two DW configurations sit with respect to the topography. There is a tall maximum at the origin, and a corrugated valley encircling it, with four low points at the VEVs. Figure 7 compares the energy densities of CoS and non-CoS domain walls.

C. Fermion zero-mode localisation

The CoS E_6 domain wall solutions described above are a good starting point for the creation of domain-wall-brane models featuring $SU(5)$-invariant effective 3 + 1-d theories for localised fields. To actually create such a

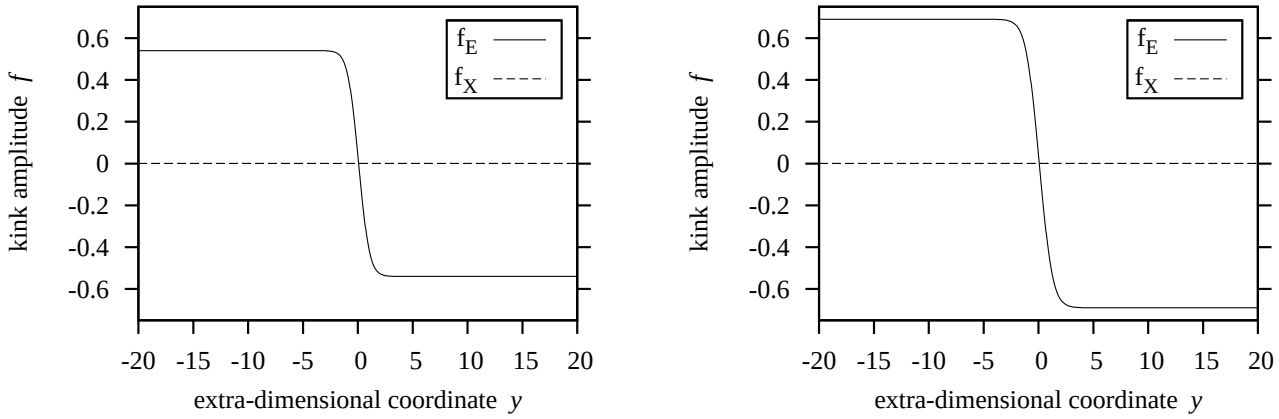

FIG. 5: Non-clash-of-symmetries domain wall solutions interpolating between $(10,+)$ at $y=-\infty$ and $(10,-)$ at $y=+\infty$. The parameters used in the left plot are $\kappa=0.2$, $\lambda_1=1.5$, $\lambda_2=0$, $\lambda_3=22.0$; those in the right plot are $\kappa=0.8$, $\lambda_1=1.0$, $\lambda_2=0$, $\lambda_3=22.0$.

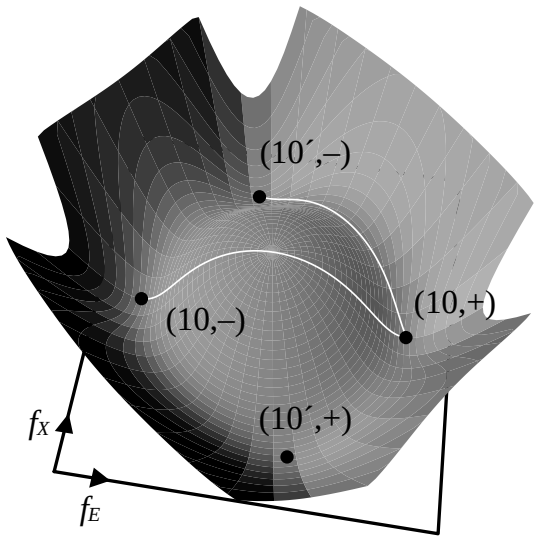

FIG. 6: Three-dimensional plot of the Higgs potential as a function of the two field components f_E and f_X. The white lines show the clash-of-symmetries domain wall (topmost) and the non-CoS domain wall (bottommost). The parameters used are $\kappa=0.8$, $\lambda_1=1.0$, $\lambda_2=0$, $\lambda_3=22.0$.

model, fermions, additional Higgs bosons and gravitons have to be added. In this subsection, we demonstrate that a phenomenologically-acceptable fermion localisation pattern is obtained using the simplest possible mechanism. We explain why this is a remarkable result.

We simply Yukawa-couple a five-dimensional fermion multiplet in the 27 of E_6,

$$\Psi \sim 27, \tag{4.41}$$

to the adjoint scalar, as per

$$\mathcal{L}_Y = -h\overline{\Psi}\chi\Psi. \tag{4.42}$$

We now substitute in the background CoS DW configuration for χ and solve the resulting Dirac equations, which take the form

$$i\Gamma^M\partial_M\Psi^{(X,E)}(x^\mu,y) - h[f_X(y)X + f_E(y)E]\Psi^{(X,E)}(x^\mu,y) = 0. \tag{4.43}$$

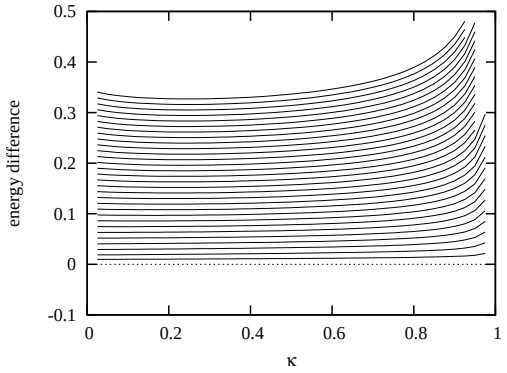

FIG. 7: The difference in energy densities between the non-CoS and CoS domain wall solutions, $E_{\rm non-CoS} - E_{\rm CoS}$. We have numerically scanned through the parameter space with $0 < \kappa < 1$ along the horizontal axis, and each successive curve represents a different λ_1, beginning at $\lambda_1 = 0.05$ at the bottom and increasing in steps of 0.05 to $\lambda_1 = 1.5$ at the top. The energy difference is always positive, so the CoS domain wall has a lower energy. We set $\lambda_2 = 0$ for simplicity.

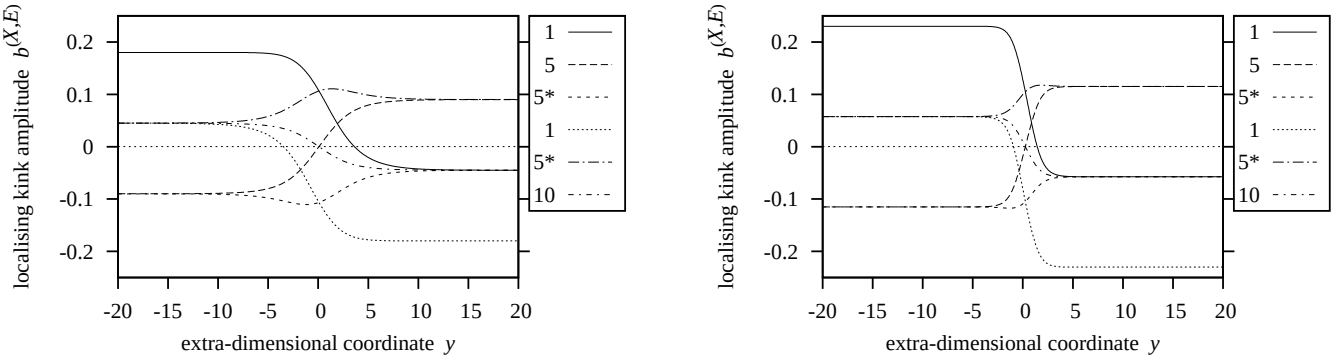

FIG. 8: Clash-of-symmetries fermion localising profiles interpolating between $(10, +)$ at $y = -\infty$ and $(10', -)$ at $y = +\infty$. The parameters used in the left plot are $\kappa = 0.2$, $\lambda_1 = 1.5$, $\lambda_2 = 0$, $\lambda_3 = 22.0$; those in the right plot are $\kappa = 0.8$, $\lambda_1 = 1.0$, $\lambda_2 = 0$, $\lambda_3 = 22.0$. The top to bottom order of the $SU(5)$ fermion multiplets in the box on the right matches the order in Eq. (4.48).

The notation $\Psi^{(X,E)}$ signifies the component of the 27 with the specified (X, E) charges, as given in Eq. (4.4). The various components couple to different background field configurations,

$$b^{(X,E)}(y) = f_X(y)X + f_E(y)E, \tag{4.44}$$

given by the DW configuration and the charges.

The Dirac matrices are $\Gamma^M = (\gamma^\mu, -i\gamma_5)$. We search for separated-variable solutions

$$\Psi(x^\mu, y) = F(y)\psi(x^\mu), \tag{4.45}$$

demanding that ψ have definite chirality, $\gamma_5\psi = \pm\psi$, and obey the $3+1$-d massless Dirac equation, $i\gamma^\mu\partial_\mu\psi = 0$. The solution for a profile is well known:

$$F^{(X,E)}(y) = N^{(X,E)}e^{-h\int^y b^{(X,E)}(y')dy'}, \tag{4.46}$$

where N is a normalisation factor. For the profile to represent localisation, it must be square-integrable with respect to y. For this to happen, $b^{(X,E)}$ must pass through zero. If so and it is an increasing function of y (kink-like), then a left-(right-)handed zero-mode occurs for $h > 0 (h < 0)$. If it passes through zero as a decreasing function (antikink-like), then a left-(right-)handed zero-mode occurs for $h < 0 (h > 0)$.

Figure 8 show the kink-like functions $b^{(X,E)}$ for the two parameter choices we have been using as examples. Let us take h to be negative:

$$h < 0. \tag{4.47}$$

Using the notation $D^{(4\sqrt{15}X,12E)}$ once again for the fermion multiplets, the following displays these functions and states the localisation outcome, which is either "localised as left-handed (LH) zero-mode" or "localised as right-handed (RH) zero-mode" or "delocalised":

$$\begin{aligned}
1^{(0,4)} &: \ \frac{1}{3}f_E, \quad \text{localised LH} \\
5^{(2,-2)} &: \ \frac{1}{2}\left(\frac{1}{\sqrt{15}}f_X - \frac{1}{3}f_E\right), \quad \text{localised RH} \\
5^{*(-2,-2)} &: \ -\frac{1}{2}\left(\frac{1}{\sqrt{15}}f_X + \frac{1}{3}f_E\right) \quad \text{delocalised} \\
1^{(-5,1)} &: \ \frac{1}{4}\left(-\frac{5}{\sqrt{15}}f_X + \frac{1}{3}f_E\right), \quad \text{localised LH} \\
5^{*(3,1)} &: \ \frac{1}{4}\left(\frac{3}{\sqrt{15}}f_X + \frac{1}{3}f_E\right), \quad \text{delocalised} \\
10^{(-1,1)}_{(-1,1)} &: \ \frac{1}{4}\left(-\frac{1}{\sqrt{15}}f_X + \frac{1}{3}f_E\right), \quad \text{localised LH.}
\end{aligned} \tag{4.48}$$

The two 5^*'s are delocalised because the associated field never goes through zero. The 5 and the 10 are localised at $y = 0$ with opposite chiralities because their background fields are kink-like and antikink-like, respectively. The two singlets are localised at nonzero y values, so the overall spectrum is "split".

This is a remarkable outcome for two reasons. First, because the 5 is localised RH, it is equivalent to a LH-localised 5^*. Thus the localised spectrum consists of LH zero-modes in the $SU(5)$ representation

$$5^* \oplus 10 \oplus 1 \oplus 1, \tag{4.49}$$

in other words one standard family plus two singlet neutrinos. Second, apart from the extra singlet, all the exotic fermions in the 27 of E_6 are delocalised and thus do not feature in the effective $3 + 1$-d theory on the brane. These benign outcomes depend crucially on the boundary condition choice embodied by the CoS domain wall solution, including the Z_2 minus sign.

Finally, there is an amusing aspect to this spectrum. It resembles a usual $SO(10)$ family plus an extra singlet. However, the LH 5^*, which is obtained from a $4 + 1$-d 5, and the 10 do not come from a 16 of either $SO(10)$ or $SO(10)'$.

V. CONCLUSION

We find it extremely encouraging that, in the E_6 context, the clash-of-symmetries idea leads to good outcomes for both gauge-boson localisation (assuming the Dvali-Shifman mechanism works) and fermion localisation; that is the main point of this paper.

In summary, we have established a general connection between the clash-of-symmetries mechanism for simultaneous brane-creation and internal-symmetry breaking with the Dvali-Shifman mechanism for gauge boson localisation. The two together provide a strong basis upon which to construct realistic domain-wall-brane models. These models should be compatible with type-2 Randall-Sundrum graviton localisation (see Ref. [16] for a CoS-style toy model featuring a background warped metric).

More specifically, we have found a domain wall solution in an E_6 adjoint-Higgs model that produces an $SU(5)\otimes U(1)^2$ symmetry on the wall itself. In one half of the bulk, the symmetry is enhanced to $SO(10) \otimes U(1)$, while in the other half of the bulk the enhancement is to $SO(10)'\otimes U(1)'$. The unprimed and primed groups are differently-embedded but

isomorphic subgroups of E_6. Because the brane-$SU(5)$ is contained in both $SO(10)$ and $SO(10)'$, the Dvali-Shifman localisation of its gauge bosons follows. The simplest possible mechanism for fermion zero-mode localisation produces a realistic spectrum, an outcome that depends on the generic features of our domain wall configuration.

To complete a realistic model, one needs to add gravity (which is expected to be straightforward) and to arrange for the additional spontaneous symmetry breaking cascade $SU(5)\otimes U(1)^2 \to SU(3)\otimes SU(2)\otimes U(1)_Y \to SU(3)\otimes U(1)_Q$. To achieve the latter, suitable additional Higgs multiplets need to be introduced, and their background field configurations have to be nonzero inside the domain wall to trigger the additional spontaneous symmetry breaking. An example of this kind of dynamical structure is described in Ref. [13], where the dominant background domain-wall configuration breaks $SU(5)$ to $SU(3)\otimes SU(2)\otimes U(1)$, and then an additional Higgs field induces electroweak symmetry breaking inside the wall.

Acknowledgments

RRV and AK were supported by the Australian Research Council, DPG by the Puzey Bequest to the University of Melbourne, and KCW in part by funds provided by the U.S. Department of Energy (D.O.E.) #DE-FG02-92ER40702. AD is supported in part by the Albert Einstein Chair in Theoretical Physics.

APPENDIX A: FULL MINIMISATION ANALYSIS

We do this in two steps. We first extend the Higgs potential minimisation analysis by adding a third adjoint component, associated with the Cartan sub-algebra generator identified as weak hypercharge Y. This is useful because the result can be graphically visualised, and it reveals a third embedding of $SO(10)$ that is related to the two embeddings used in the main body of the text. In the second step, we report on a numerical study of the whole six-dimensional Cartan subspace.

The truncated multiplet is thus first increased to

$$\chi = f_E E + f_X X + f_Y Y, \tag{A1}$$

where

$$\begin{aligned}
E &= \frac{1}{12}\mathrm{diag}(4,-2,-2,-2,-2,-2,-2,-2,-2,-2,-2,1,1,1,1,1,1,1,1,1,1,1,1,1,1,1,1,1),\\
X &= \frac{1}{4\sqrt{15}}\mathrm{diag}(0,2,2,2,2,2,2,-2,-2,-2,-2,-2,-5,3,3,3,3,3,-1,-1,-1,-1,-1,-1,-1,-1,-1,-1),\\
Y &= \frac{1}{2\sqrt{10}}\mathrm{diag}\left(0,1,1,-\frac{2}{3},-\frac{2}{3},-\frac{2}{3},-1,-1,\frac{2}{3},\frac{2}{3},0,-1,-1,\frac{2}{3},\frac{2}{3},\frac{2}{3},\frac{1}{3},\frac{1}{3},\frac{1}{3},\frac{1}{3},\frac{1}{3},\frac{1}{3},\frac{1}{3},-\frac{4}{3},-\frac{4}{3},-\frac{4}{3},2\right),
\end{aligned} \tag{A2}$$

have been normalised as per

$$\mathrm{Tr}(E^2) = \mathrm{Tr}(X^2) = \mathrm{Tr}(Y^2) = 1/2, \qquad \mathrm{Tr}(EX) = \mathrm{Tr}(EY) = \mathrm{Tr}(XY) = 0. \tag{A3}$$

The sextic invariant is

$$I_6 = \mathrm{Tr}[(f_E E + f_X X + f_Y Y)^6]. \tag{A4}$$

To visualise its structure, we go to a spherical-polar decomposition

$$f_E \equiv r\sin\phi\cos\theta, \quad f_X \equiv r\sin\phi\sin\theta, \quad f_Y \equiv r\cos\phi, \tag{A5}$$

which produces

$$\begin{aligned} I_6 &= \frac{r^6}{518400}\Big(710\cos^6\phi + 30\cos^4\phi\left(51+4\cos 2\theta - 4\sqrt{15}\sin 2\theta\right)\sin^2\phi \\ &+ 60\sqrt{2}\cos^3\phi\sin\theta\left(2\sqrt{3}+3\sqrt{3}\cos 2\theta - \sqrt{5}\sin 2\theta\right)\sin^3\phi \\ &- 45\cos^2\phi\left(-34+2\cos 2\theta + 7\cos 4\theta - 2\sqrt{15}\sin 2\theta + \sqrt{15}\sin 4\theta\right)\sin^4\phi \\ &+ \frac{3}{2}\left(440+15\cos 2\theta + 84\cos 4\theta + 11\cos 6\theta - 15\sqrt{15}\sin 2\theta + 12\sqrt{15}\sin 4\theta - 3\sqrt{15}\sin 6\theta\right)\sin^6\phi \\ &+ 144\cos^5\phi\left(\sqrt{10}\cos\theta\sin\phi - \sqrt{6}\sin\theta\sin\phi\right)\Big) \end{aligned} \tag{A6}$$

Figure 9 plots $-I_6/r^6$ as a function of θ and ϕ. The (E,X) plane is the line $\phi=\pi/2$, along which the VEVs $(10,\pm)$ and $(10',\pm)$ can be seen. Degenerate with them are two more VEVs with $f_Y\neq 0$, located at

$$\theta = \arccos\left(-\frac{1}{2}\sqrt{\frac{5}{2}}\right), \quad \phi = \arccos\left(-\frac{3}{\sqrt{10}}\right) \tag{A7}$$

and

$$\theta = -\arccos\left(\frac{1}{2}\sqrt{\frac{5}{2}}\right), \quad \phi = \arccos\left(\frac{3}{\sqrt{10}}\right). \tag{A8}$$

The first VEV corresponds to a nonzero value for the adjoint component associated with the generator $-E''$, where

$$E'' = \frac{1}{4}E - \frac{1}{4}\sqrt{\frac{3}{5}}X + \frac{3}{\sqrt{10}}Y. \tag{A9}$$

As the notation suggests, this minimum breaks E_6 to yet a third differently-embedded subgroup which we can call $SO(10)''\otimes U(1)_{E''}$, with negative Z_2 parity: $(10'',-)$. The second VEV is just $(10'',+)$.

The three groups $SO(10)$, $SO(10)'$ and $SO(10)''$ share a common $SU(3)\otimes SU(2)$ subgroup, but the $SU(5)$ contained in $SO(10)\cap SO(10)'$ is *not* a subgroup of $SO(10)''$ (this is obvious, since E'' contains an admixture of Y which is a generator of that $SU(5)$). One can imagine a domain-wall junction configuration that utilises all three of these embeddings for boundary conditions, but such a model would have a similar photon and Z-boson leakage problem as the warm-up example of Sec. III.

The functions $-I_8/r^8$, $-(I_5)^2/r^{10}$ and $-I_{12}/r^{12}$ have exactly the same qualitative structure as $-I_6/r^6$. Thus $(10,\pm)$, $(10',\pm)$ and $(10'',\pm)$ will be the degenerate global minima for a large class of potentials. The quadratic invariant is θ,ϕ-independent,

$$I_2 = \frac{1}{2}(f_E^2 + f_X^2 + f_Y^2) \tag{A10}$$

so one can simply add appropriate $(I_2)^n$ terms to the potential to ensure it is bounded from below, and to generate a definite value for r at the global minima. The positions of the global minima are determined entirely from the angular structure of the non-isotropic terms.

One can extend the analysis to all six Cartan components using a six-dimensional hyperspherical polar decomposition. The six fields are represented by one modulus, r, four zenith angles $0\leq\phi_{1,2,3,4}\leq\pi$ and one azimuthal angle $-\pi\leq\theta<\pi$. Because the group theoretic character of an extremum is determined entirely from the angular structure of the invariants, a numerical study can readily be performed on the finite domain $(\phi_{1,2,3,4},\theta)$. This study confirmed that the $E_6\to SO(10)\otimes U(1)$ VEVs are the global minima of $-I_{6,8,12}$ and $-(I_5)^2$. The additional field dimensions simply revealed more degenerate vacua, corresponding to extra embeddings of $SO(10)$ in E_6. These new embeddings must correspond, physically speaking, to choosing different $SU(3)\otimes SU(2)$ subgroups for colour and isospin. The total number of $E_6\to SO(10)\otimes U(1)$ extrema was found to be 54, consisting of 27 Z_2-related pairs. This implies that, overall, there are 27 embeddings of $SO(10)\otimes U(1)$ in E_6. Though we shall not display the results here, we

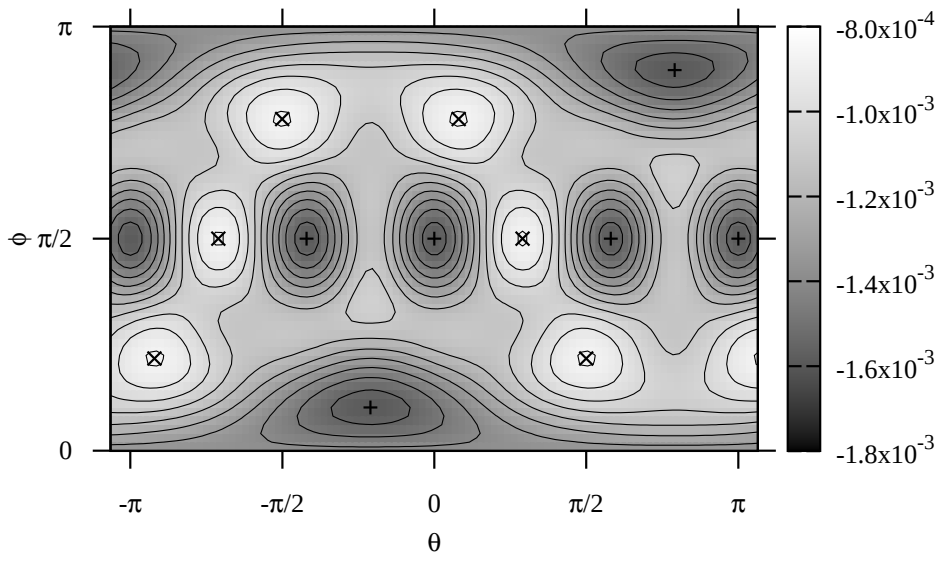

FIG. 9: Contour plot of $-I_6/r^6$ as a function of θ and ϕ. The degenerate global minima breaking E_6 to various $SO(10) \otimes U(1)$ subgroups are marked with + signs, while the local maxima are indictaed with $\times$ signs. The row of minima along $\phi = \pi/2$ correspond to the global minima displayed in Fig. 2.

have analytical expressions for the 27 linear combinations of Cartan generators that correspond to these VEVs. In the breakdown $27 \to 1 \oplus 10 \oplus 16$, these 27 linear combinations turn out to be correlated with the choice of which component to assign as the $SO(10)$ singlet in the decomposition. A deeper reason for the number 27 is perhaps the following: according to the $SU(3) \otimes SU(3) \otimes SU(3)$ maximal subgroup of E_6, there are three independent choices for the colour group. The weak-isospin group can then be selected as the $I-$, $U-$ or $V-$spin subgroup of either of the two remaining $SU(3)$'s. This gives $3 \times 6 = 18$ choices for $SU(3) \otimes SU(2)$ embeddings. According to our previous analysis, each $SU(3) \otimes SU(2)$ is contained in the intersection of three different $SO(10)$'s, which suggests there should be $18 \times 3 = 54$ embeddings of $SO(10)$. However, recognising that $SO(10)$ contains an $SU(2) \otimes SU(2)$ subgroup, we see that the correct number of independent embeddings is actually $54/2 = 27$.

[1] V. A. Rubakov and M. E. Shaposhnikov, Phys. Lett. **B125**, 136 (1983).
[2] K. Akama, Lecture Notes in Physics, Berlin Springer-Verlag **176**, 267 (1983).
[3] M. Visser, Phys. Lett. **B159**, 22 (1985).
[4] G. W. Gibbons and D. L. Wiltshire, Nucl. Phys. **B287**, 717 (1987).
[5] N. Arkani-Hamed, S. Dimopoulos, and G. R. Dvali, Phys. Lett. **B429**, 263 (1998).
[6] I. Antoniadis, Phys. Lett. **B246**, 377 (1990).
[7] I. Antoniadis, N. Arkani-Hamed, S. Dimopoulos, and G. Dvali, Phys. Lett. **B436**, 257 (1998).
[8] L. Randall and R. Sundrum, Phys. Rev. Lett. **83**, 3370 (1999).
[9] L. Randall and R. Sundrum, Phys. Rev. Lett. **83**, 4690 (1999).
[10] M. Gremm, Phys. Lett. **B478**, 434 (2000).
[11] O. DeWolfe, D. Z. Freedman, S. S. Gubser, and A. Karch, Phys. Rev. **D62**, 046008 (2000).
[12] A. Davidson and P. D. Mannheim (2000), hep-th/0009064.
[13] R. Davies, D. P. George, and R. R. Volkas (2007), arXiv:0705.1584[hep-ph].
[14] A. Davidson, B. F. Toner, R. R. Volkas, and K. C. Wali, Phys. Rev. **D65**, 125013 (2002).

[15] J. S. Rozowsky, R. R. Volkas, and K. C. Wali, Phys. Lett. **B580**, 249 (2004).
[16] G. Dando, A. Davidson, D. P. George, R. R. Volkas, and K. C. Wali, Phys. Rev. **D72**, 045016 (2005).
[17] E. M. Shin and R. R. Volkas, Phys. Rev. **D69**, 045010 (2004).
[18] L. Pogosian and T. Vachaspati, Phys. Rev. **D62**, 123506 (2000).
[19] T. Vachaspati, Phys. Rev. **D63**, 105010 (2001).
[20] L. Pogosian and T. Vachaspati, Phys. Rev. **D64**, 105023 (2001).
[21] G. Dvali and M. Shifman, Nucl. Phys. **B504**, 127 (1997).
[22] G. R. Dvali and M. A. Shifman, Phys. Lett. **B396**, 64 (1997).
[23] R. Jackiw and C. Rebbi, Phys. Rev. **D13**, 3398 (1976).
[24] V. A. Rubakov, Phys. Usp. **44**, 871 (2001).
[25] M. Creutz, Phys. Rev. Lett. **43**, 553 (1979).
[26] G. 't Hooft, in *High Energy Physics*, Proceedings of the EPS International Conference, Palermo 1975, ed. A Zichichi, Editrice Compositori, Bologna (1976).
[27] S. Mandelstam, Phys. Rep. **C23**, 245 (1976).
[28] N. Arkani-Hamed and M. Schmaltz, Phys. Lett. **B450**, 92 (1999).
[29] S. L. Dubovsky and V. A. Rubakov, Int. J. Mod. Phys. **A16**, 4331 (2001).
[30] A. Demaria and R. R. Volkas, Phys. Rev. **D71**, 105011 (2005).
[31] E. Dynkin, Mat. Sb. **30**, 349 (1952).
[32] L.-F. Li, Phys. Rev. **D9**, 1723 (1974).
[33] O. Kaymakcalan, L. Michel, K. C. Wali, W. D. McGlinn, and L. O'Raifeartaigh, Nucl. Phys. **B267**, 203 (1986).
[34] M. Bando and T. Kugo, Prog. Theor. Phys. **101**, 1313 (1999).
[35] M. Bando, T. Kugo, and K. Yoshioka, Prog. Theor. Phys. **104**, 211 (2000).
[36] G. W. Anderson and T. Blazek, J. Math. Phys. **41**, 4808 (2000).
[37] N. Maekawa and T. Yamashita, Phys. Lett. **B567**, 330 (2003).
[38] G. Racah, Lincei. Rend. Sci. Fis. Mat. Nat. **8**, 108 (1950).
[39] J. A. Harvey, Nucl. Phys. **B163**, 254 (1980).